Supporting Information. Holly V. Moeller, Michael G. Neubert, and Matthew D. Johnson. 2019. Intraguild predation enables coexistence of competing phytoplankton in a well-mixed water column. *Ecology*.

Appendix S1: Supplemental Tables and Figures

Table S1: Media Nutrient Content

Component	Concentration in K medium* (used for stock cultures)	Concentration in 2K medium** (used for comparative experiment)
$NaNO_3$	$8.82x10^{-4}$ M	$1.76x10^{-3}$ M
NH_4Cl	$5.00x10^{-5}$ M	$1.00x10^{-4}$ M
Na_2 *b*-glycerophosphate	$1.00x10^{-5}$ M	$2.00x10^{-5}$ M
$Na_2SiO_3 \cdot 9H_2O$	$5.04x10^{-4}$ M	$1.01x10^{-3}$ M
H_2SeO_3	$1.00x10^{-8}$ M	$2.00x10^{-8}$ M
Tris-base (pH 7.2)	$1.00x10^{-3}$ M	$2.00x10^{-3}$ M
$Na_2EDTA \cdot 2H_2O$	$1.11x10^{-4}$ M	$2.22x10^{-4}$ M
$FeCl_3 \cdot 6H_2O$	$1.17x10^{-5}$ M	$2.34x10^{-5}$ M
$MnCl_2 \cdot 4H_2O$	$9.00x10^{-7}$ M	$1.80x10^{-6}$ M
$ZnSO_4 \cdot 7H_2O$	$8.00x10^{-8}$ M	$1.60x10^{-7}$ M
$CoCl_2 \cdot 6H_2O$	$5.00x10^{-8}$ M	$1.00x10^{-7}$ M
$Na_2MoO_4 \cdot 2H_2O$	$2.60x10^{-8}$ M	$5.20x10^{-8}$ M
$CuSO_4 \cdot 5H_2O$	$1.00x10^{-8}$ M	$2.00x10^{-8}$ M
thiamine · HCl (vit. B_1)	$2.96x10^{-7}$ M	$5.92x10^{-7}$ M
biotin (vit. H)	$2.05x10^{-9}$ M	$4.10x10^{-9}$ M
cyanocobalamin (vit. B_{12})	$3.69x10^{-10}$ M	$7.38x10^{-10}$ M
Total N	$9.32x10^{-4}$ M	$1.86x10^{-3}$ M
Total P	$1.00x10^{-5}$ M	$2.00x10^{-5}$ M

*Concentrations listed below are provided by the National Center for Marine Algae and Microbiota based on the use of their K medium kit. Kits are designed to recapitulate the media described by Keller et al. (1987). Kit nutrients were added to autoclaved, 0.2μm-filtered Santa Barbara Coastal Seawater. Because coastal seawater is usually relatively replete in inorganic nutrients, actual concentrations in the growth media were likely higher than listed in the table.

**2K medium was made by adding double the amount of nutrients per liter of seawater called for in the K medium kit; thus, estimated nutrient concentrations are double that in typical K medium.

Table S2: Cellular Nutrient Content

Species	Carbon per cell $f$mol/cell	Nitrogen per cell $f$mol/cell	Phosphorus per cell $f$mol/cell	Source
Micromonas	146	14.8	0.18	(Maat et al., 2014)
Ochromonas 1391	4973	705		(Verity et al., 1992)
Ochromonas 1393	2133	310		(Verity et al., 1992)
Ochromonas 2951	3505	502		(Verity et al., 1992)

Table S3: Nutrient Budget

Experiment	*Micromonas* Abundance (cells/mL)	*Ochromonas* Abundance (cells/mL)	Carbon (M)	Nitrogen (M)	Phosphorus (M)	% N remaining	% P remaining
Fresh media				$1.86\text{x}10^{-3}$	$2.00\text{x}10^{-5}$	100	100
Micromonas	$4.80\text{x}10^{6}$		$7.01\text{x}10^{-4}$	$7.11\text{x}10^{-5}$	$9.00\text{x}10^{-7}$	96.2	95.5
Och. 1391		$3.80\text{x}10^{5}$	$1.89\text{x}10^{-3}$	$2.68\text{x}10^{-4}$		85.6	
Och. 1393		$2.72\text{x}10^{5}$	$5.80\text{x}10^{-4}$	$8.42\text{x}10^{-5}$		95.5	
Och. 2951		$1.49\text{x}10^{6}$	$5.22\text{x}10^{-3}$	$7.47\text{x}10^{-4}$		59.9	
Mic. + *Och.* 1391	$4.84\text{x}10^{6}$	$4.06\text{x}10^{5}$	$2.72\text{x}10^{-3}$	$3.57\text{x}10^{-4}$		80.8	
Mic. + *Och.* 1393	0	$2.61\text{x}10^{5}$	$5.57\text{x}10^{-4}$	$8.10\text{x}10^{-5}$		95.7	
Mic. + *Och.* 2951	$1.40\text{x}10^{6}$	$1.18\text{x}10^{6}$	$4.34\text{x}10^{-3}$	$6.13\text{x}10^{-4}$		67.1	

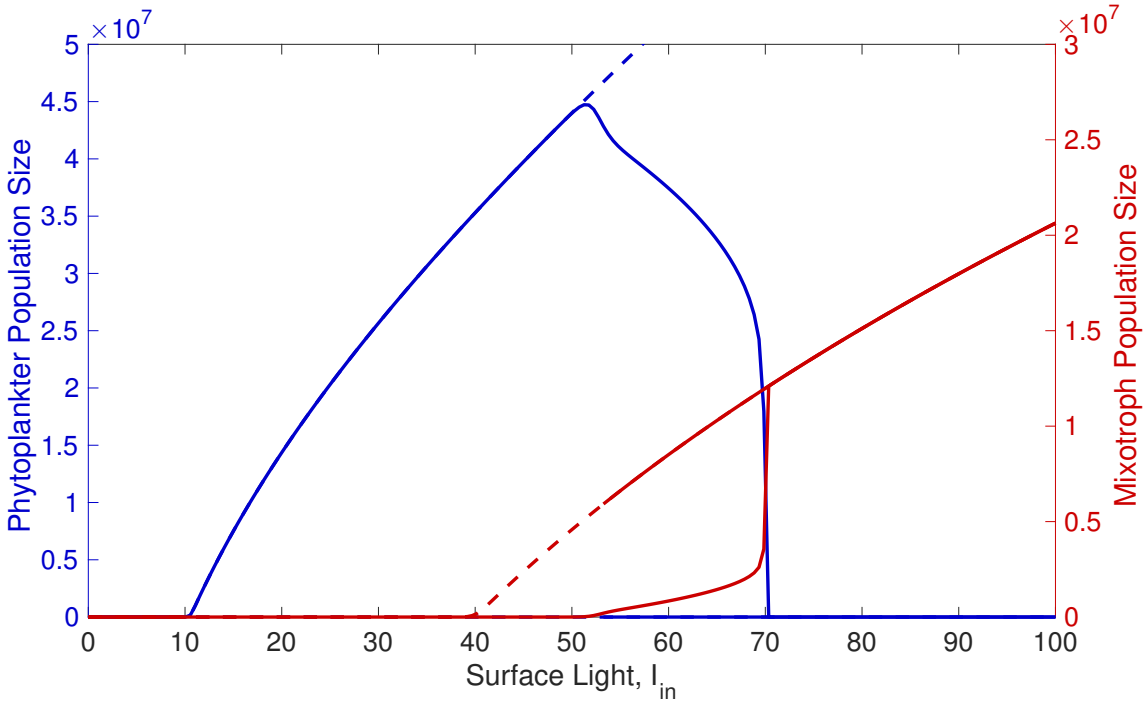

Figure S1: Response of population sizes of the phytoplankter (blue) and mixotroph (red) to surface incoming light (x-axis). Once light increases above I_W, the compensation irradiance for the phytoplankter, the phytoplankter persists in isolation, with a carrying capacity that increases monotonically with surface light input. The phytoplankter's superior competitive ability for light prevents the invasion of the mixotroph, although it could persist in isolation (dashed red line), until light levels are sufficiently high for coexistence ($I_{in} > 51$). The system becomes bistable when I_{in} exceeds 54: Depending upon initial conditions, the mixotroph either coexists with, or competitively excludes, the phytoplankter. For much higher surface irradiances ($I_{in} > 70$), the mixotroph competitively excludes the phytoplankter regardless of initial conditions. Parameters are listed in Table 1, with $p_m = 0.3$, $h_m = 200$, $\ell_m = 0.05$, $k_m = 1x10^{-7}$, $a = 2x10^{-8}$, and $b = 0.04$.

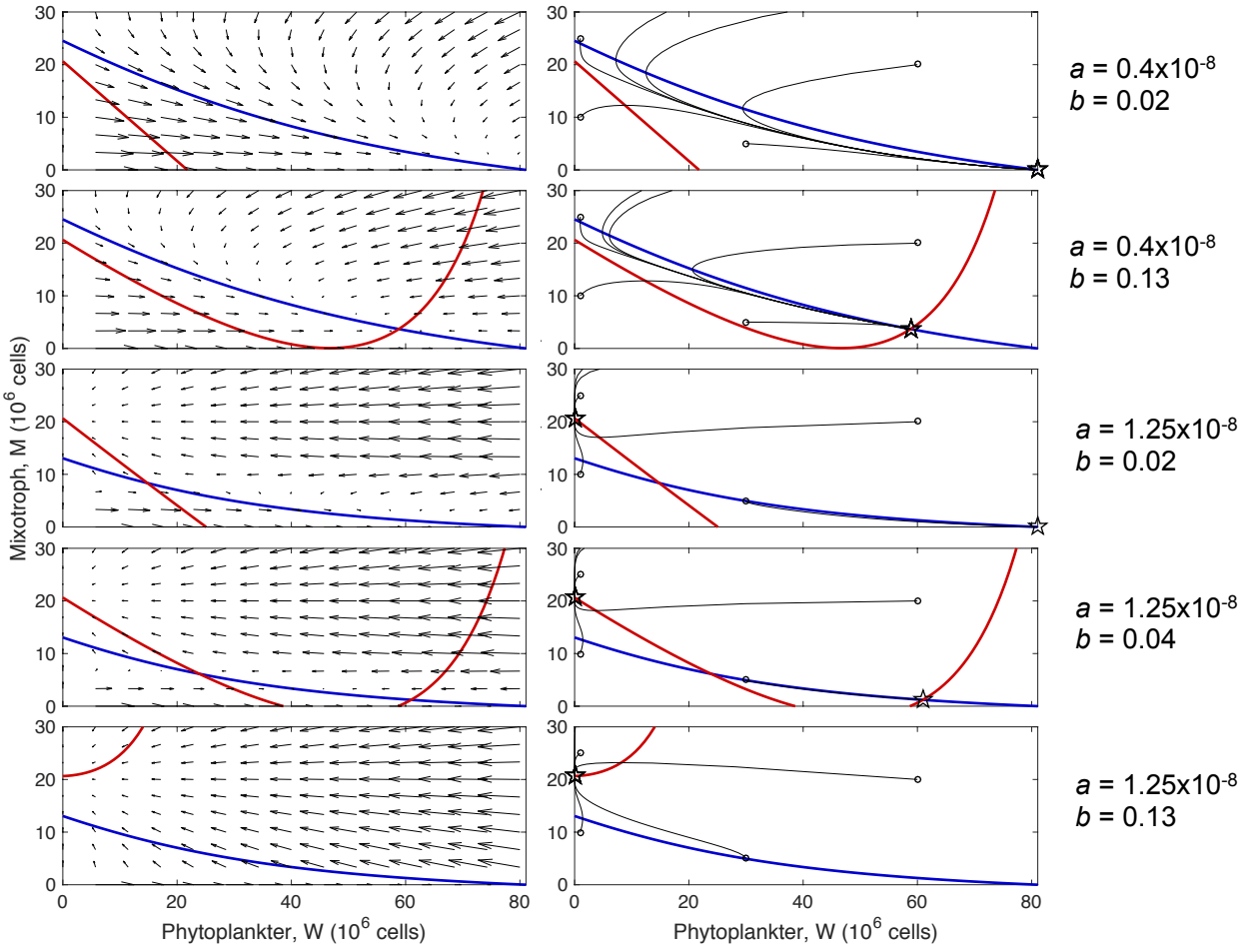

Figure S2: Zero net growth nullclines for the phytoplankter W in blue and the mixotroph M in red, for five different sets of a and b (different rows, as in Figure 1). Nullcline plots are underlaid by a velocity field (left column) indicating short-term changes in population sizes for various initial conditions, or by five example population trajectories (right column) indicating how populations change over time from initial conditions (indicated by circles) to equilibrium states (stars). Parameters are listed in Table 1, with $p_m = 0.3$, $h_m = 200$, $\ell_m = 0.05$.

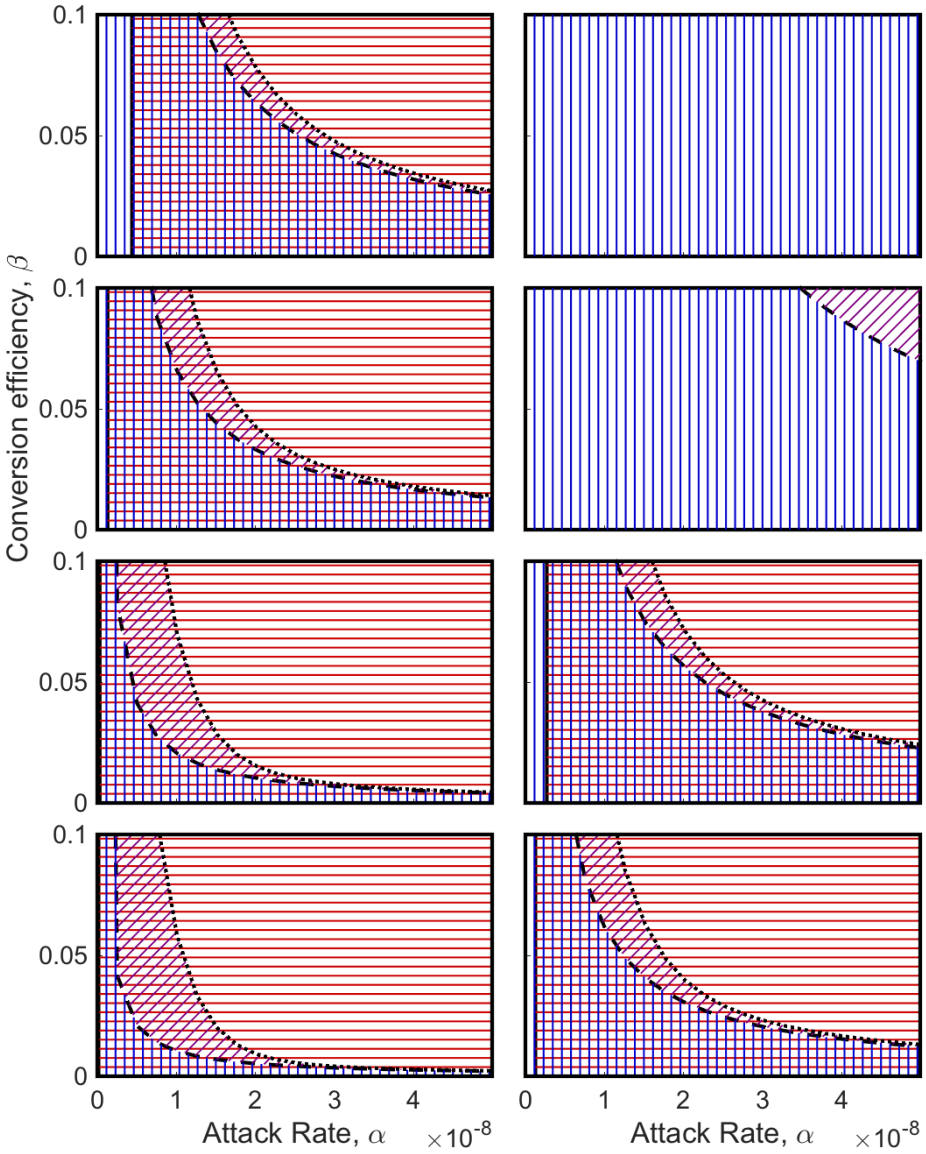

Figure S3: Effects of input light and trait differences on the stability of model equilibria as a function of attack rate a and conversion efficiency b parameter space. Surface light I_{in} is set at 15, 20, 50, and 100 for the first, second, third, and fourth rows respectively. For the left column, the phytoplankter and mixotroph differ only in half-saturation constants ($h_m = 250$; $\ell_m = 0.05$). For the right column, the phytoplankter and mixotroph differ in mortality rates ($\ell_m = 0.1$; $h_m = 200$). All other parameters are listed in Table 1, with $p_m = 1$ and $k_m = 1x10^{-7}$. Stability regions are colored and hatched as in Figure 1.

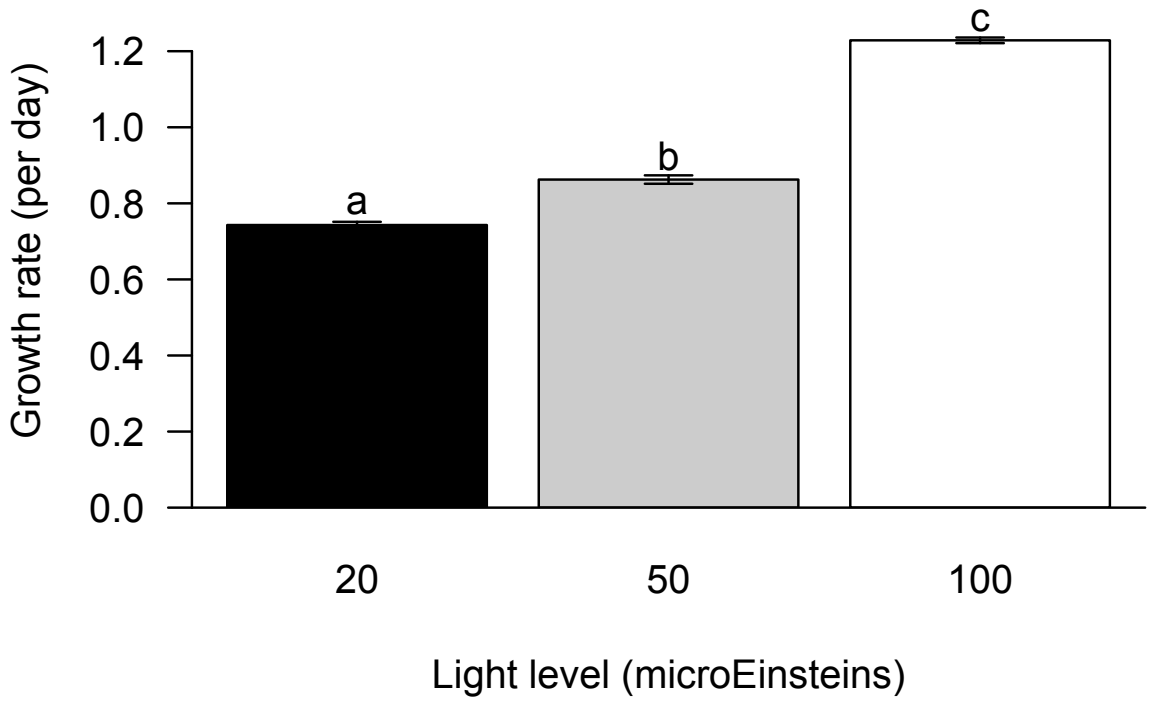

Figure S4: Growth rate of *Micromonas* as a function of light. Initial growth rates were measured over the first 24 hours of the main experiment, in order to reduce the effects of intraspecific competition as population sizes increased. *Micromonas*'s growth rate increased with increasing availability of light. Bar heights represent means; whiskers indicate 95% confidence intervals. Letters indicate significant differences at the $p < 0.001$ level (Tukey's HSD comparing population size grouped by *Ochromonas* strain).

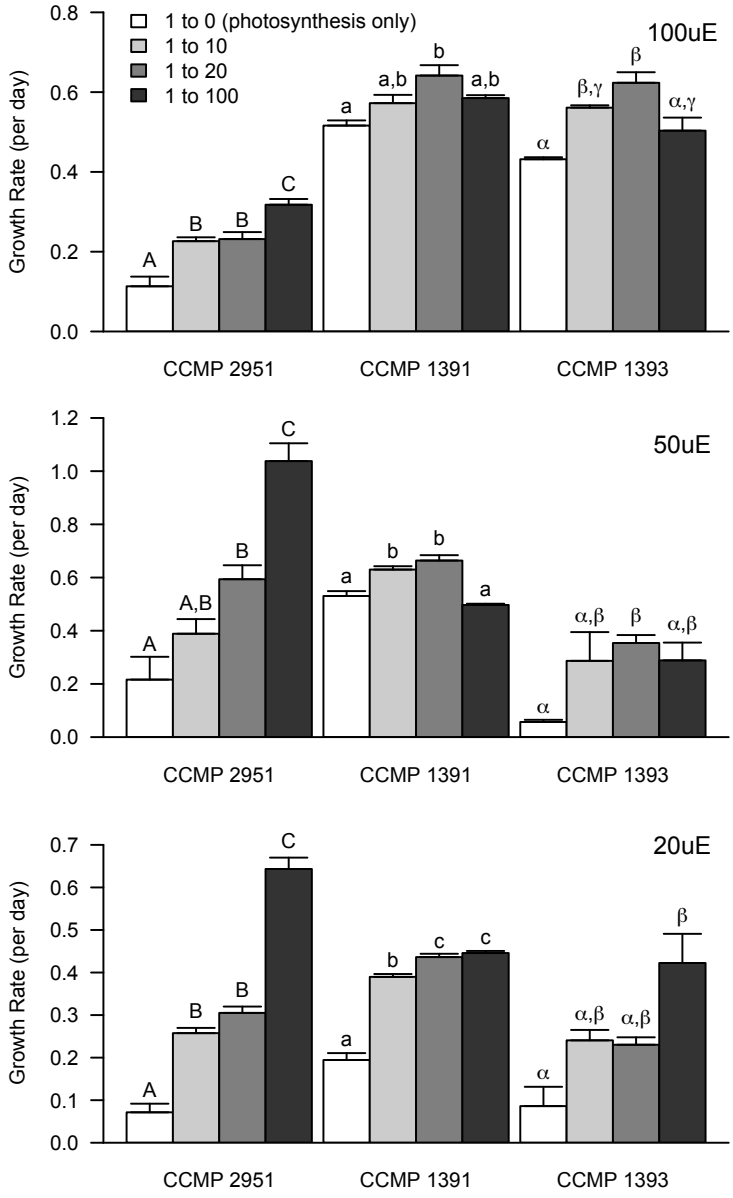

Figure S5: Mixotrophic growth response of *Ochromonas*. Initial growth rates were measured over the first 24 hours of the main experiment, in order to reduce the effects of competition as population sizes increased. *Ochromonas*'s mixotrophic growth rate increased with increasing availability of the phytoplankter prey species *Micromonas*. Data are shown for four initial prey concentrations ranging from no prey (i.e., 0 initial *Micromonas* cells/mL, so that all measured growth is photosynthetic; white bars) to high prey (i.e., 200,000 initial *Micromonas* cells/mL; dark gray bars). Bar heights represent means; whiskers indicate 95% confidence intervals. Letters indicate significant differences at the $p < 0.05$ level (Tukey's HSD comparing population size grouped by *Ochromonas* strain).

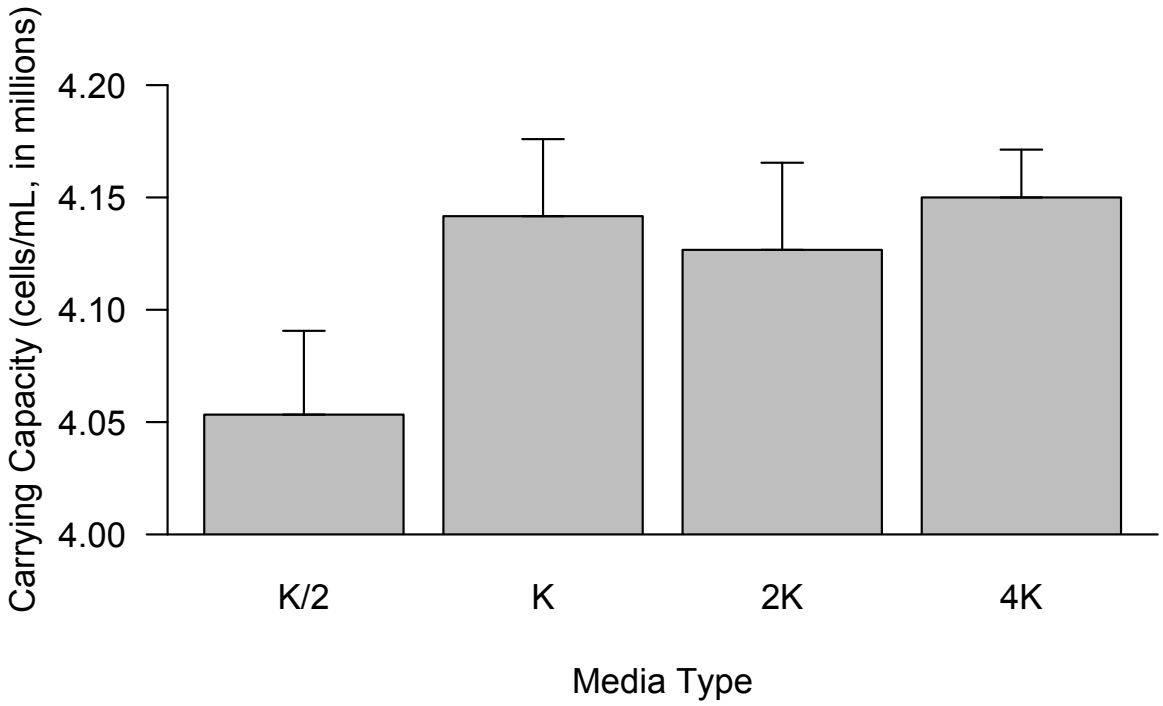

Figure S6: Carrying capacity of *Micromonas* grown in media with varied nutrient content. We observed no significant differences in carrying capacity across four nutrient conditions (Tukey's HSD, $p > 0.05$). Although carrying capacity was lower for K/2 media, this difference was not significant. Bar heights represent means; whiskers indicate 95% confidence intervals. Data are from a pilot experiment.

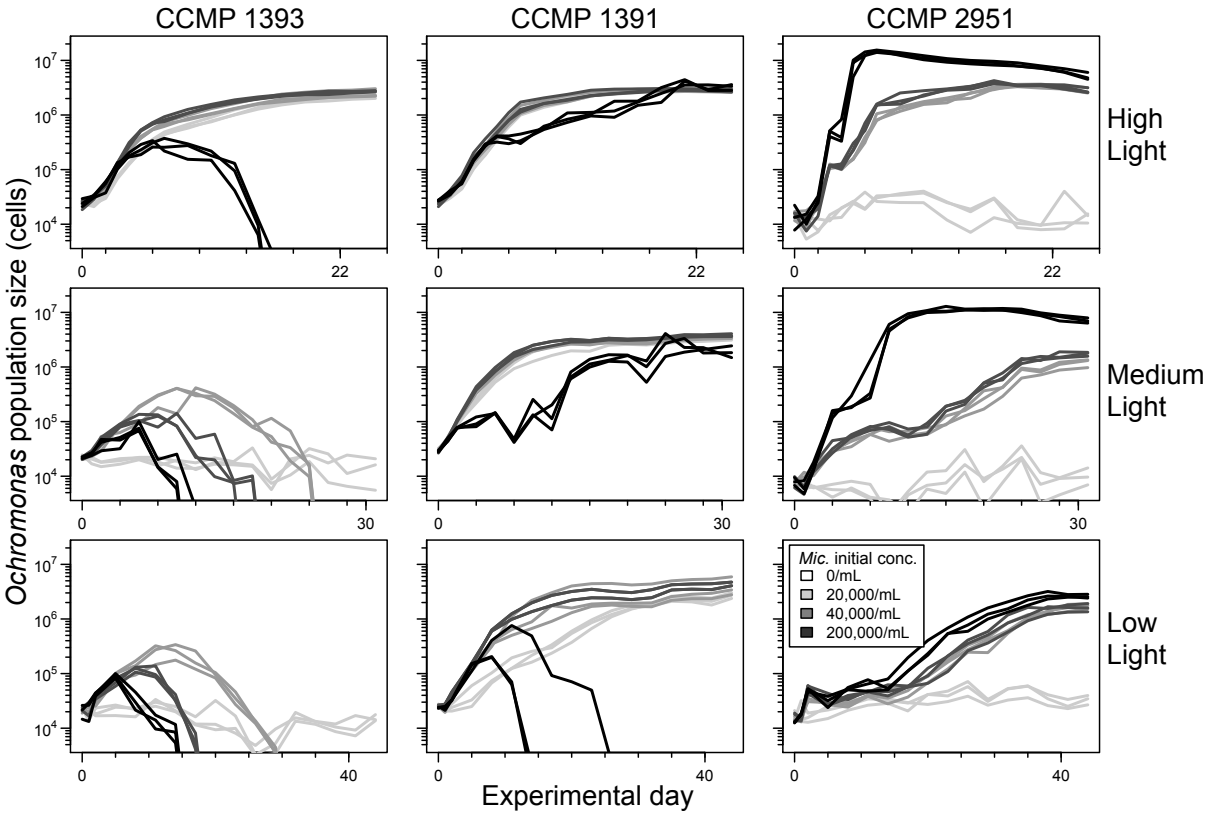

Figure S7: Individual replicate population trajectories of *Ochromonas* by light level (different rows), strain (different columns), and initial conditions (grayscale; see legend in bottom right panel) in the main experiment.

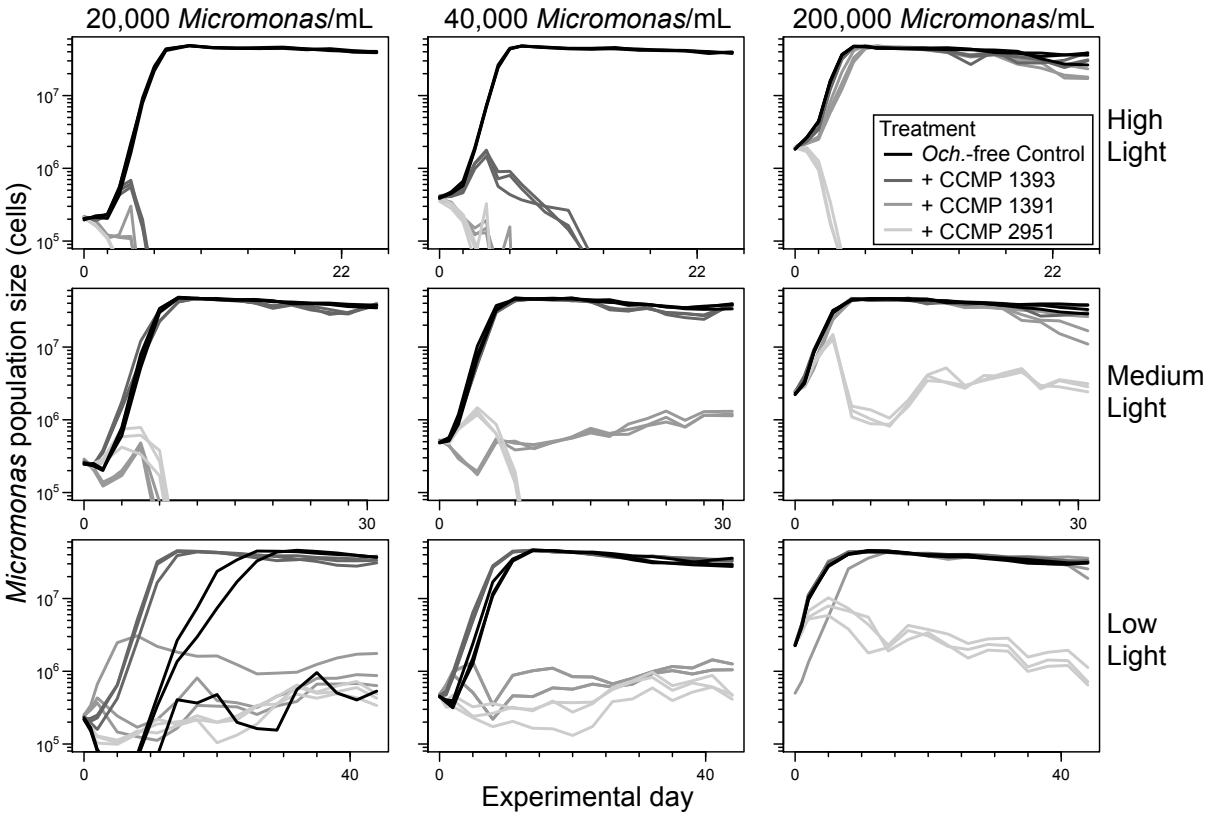

Figure S8: Individual replicate population trajectories of *Micromonas* grown in co-culture with *Ochromonas*, grouped by light level (different rows), initial condition (different columns), and *Ochromonas* strain (grayscale; see legend in upper right panel) in the main experiment. For reference, controls (*Ochromonas*-free growth curves) for each experimental treatment are plotted in black.

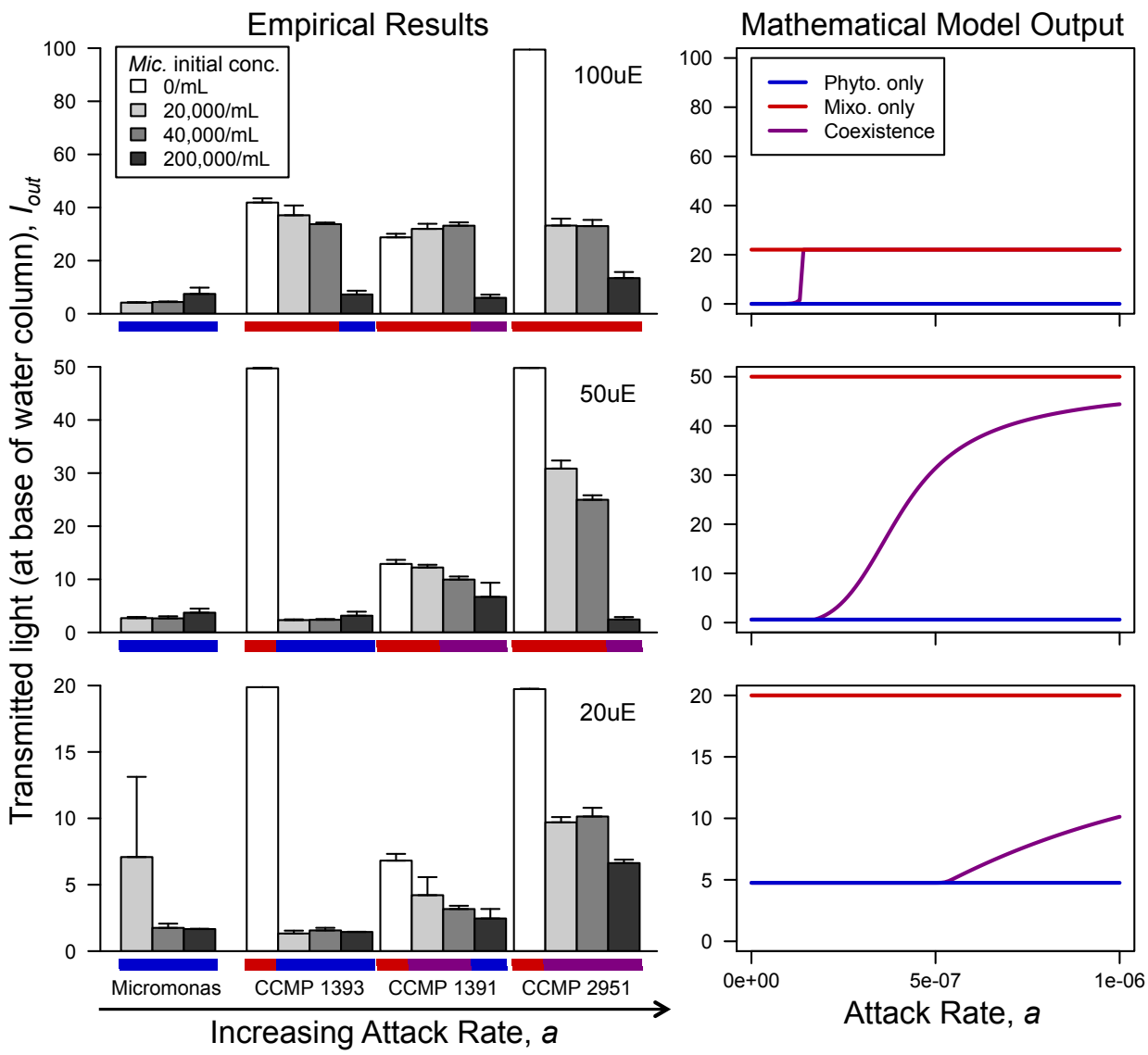

Figure S9: Transmitted light (I_{out}) calculated for the end of the main laboratory experiment (left column) and predicted by the mathematical model (right column). Results are shown for all three experimental light levels (top row: 100 $\mu mol\ quanta\ m^{-2}\ s^{-1}$; middle row: 50 $\mu mol\ quanta\ m^{-2}\ s^{-1}$; bottom row: 20 $\mu mol\ quanta\ m^{-2}\ s^{-1}$). For the empirical results, bar heights represent means; whiskers indicate 95% confidence intervals. Results are shown for *Micromonas* alone (leftmost set of bars) and for all three strains of *Ochromonas*. Bar shading represents initial inoculation concentration of *Micromonas* (see legend; for *Micromonas*-only treatments, *Ochromonas* was not inoculated). Color bars below the x-axis indicate the equilibrium outcome (blue: *Micromonas* only; red: *Ochromonas*-only; purple: coexistence). For the mathematical results, parameters are set as in Figure 4: $p_m = 0.3$, $h_m = 250$, $\ell_m = 0.1$, and $k_m = 5x10^{-7}$.

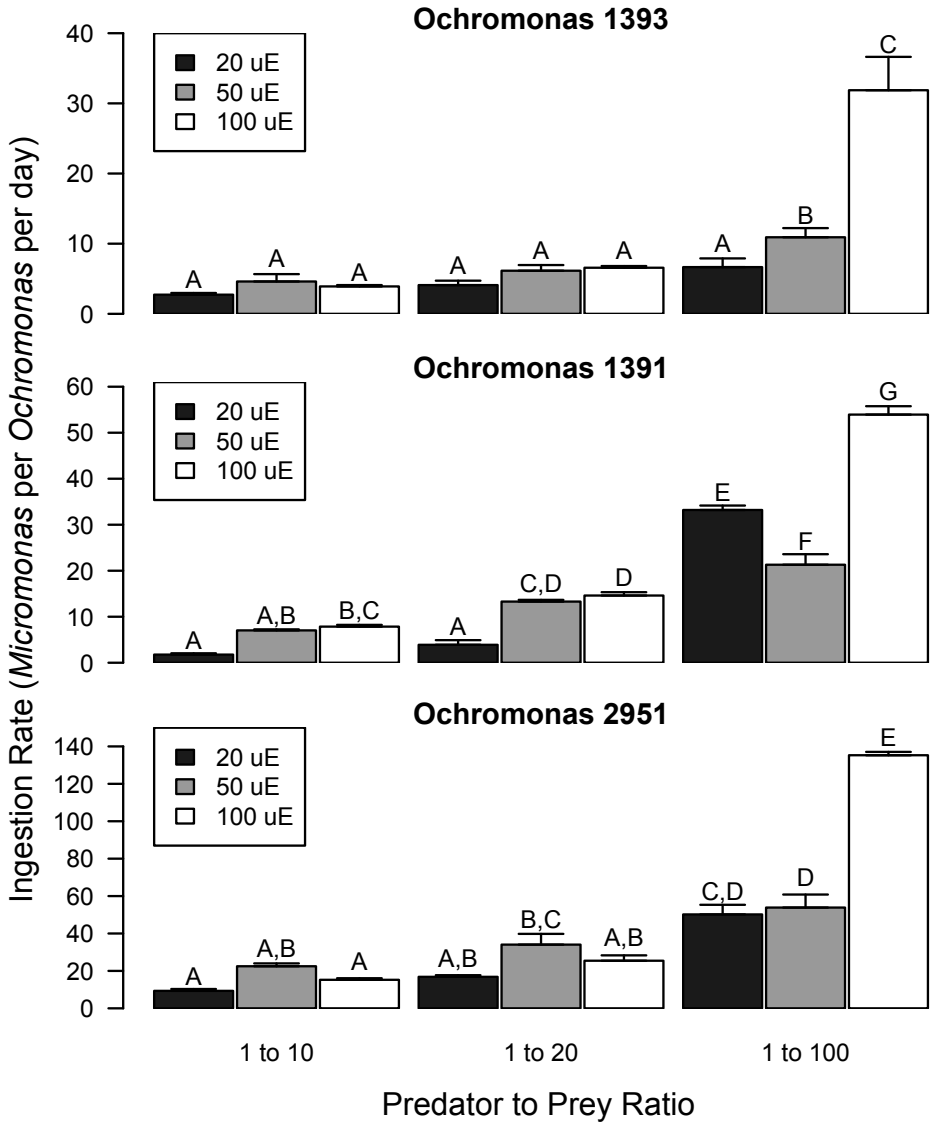

Figure S10: Grazing rates of *Ochromonas* on *Micromonas* by prey initial concentration and experimental light level. Bar heights represent means, whiskers indicate 95% confidence intervals, and different letters indicate treatments with statistically significantly different means (Tukey's HSD, $p < 0.05$). In general, grazing rates increased with increasing prey availability (from left to right), with CCMP 2951 having the highest grazing rates overall (note different y-axis scales). While grazing rates did tend to increase with increasing light, this trend was not consistent across all treatments. Data are from a preliminary experiment designed to specifically quantify grazing rates.